Electronic Supplementary Material (ESI) for Journal of Materials Chemistry A.

Electronic Supplementary Information

A Controllable Strategy for the Self-Assembly of WM Nanocrystals/Nitrogen-Doped Porous Carbon Superstructure (M = O, C, P, S, and Se) for Sodium and Potassium Storage

Xiaojuan Jiao[ac], Xiaojie Liu[ac], Beibei Wang[bc*], Gang Wang[bc], Hui Wang[ac*]

[a]*Key Laboratory of Synthetic and Natural Functional Molecule Chemistry (Ministry of Education), College of Chemistry & Materials science, Northwest University, Xi'an 710127, PR China*

[b]*State Key Lab Incubation Base of Photoelectric Technology and Functional Materials, International Collaborative Center on Photoelectric Technology and Nano Functional Materials, Institute of Photonics & Photon-Technology, Northwest University, Xi'an 710069, PR China*

[c]*Shaanxi Joint Lab of Graphene (NWU), Xi'an 710127, PR China*

[*]Corresponding author:

Tel.: +86 029 8836 3115

Fax: +86 029 8830 3798

E-mail address: huiwang@nwu.edu.cn (H. Wang), beibeiwang@nwu.edu.cn

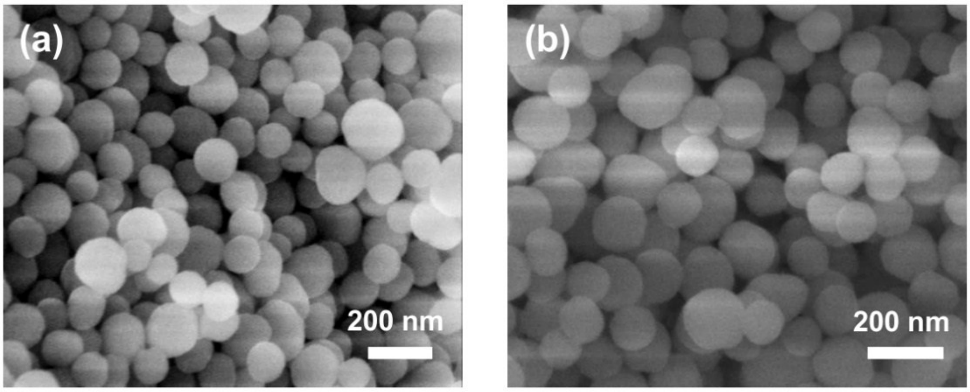

Figure S1 SEM images of SiO_2@C solid spheres.

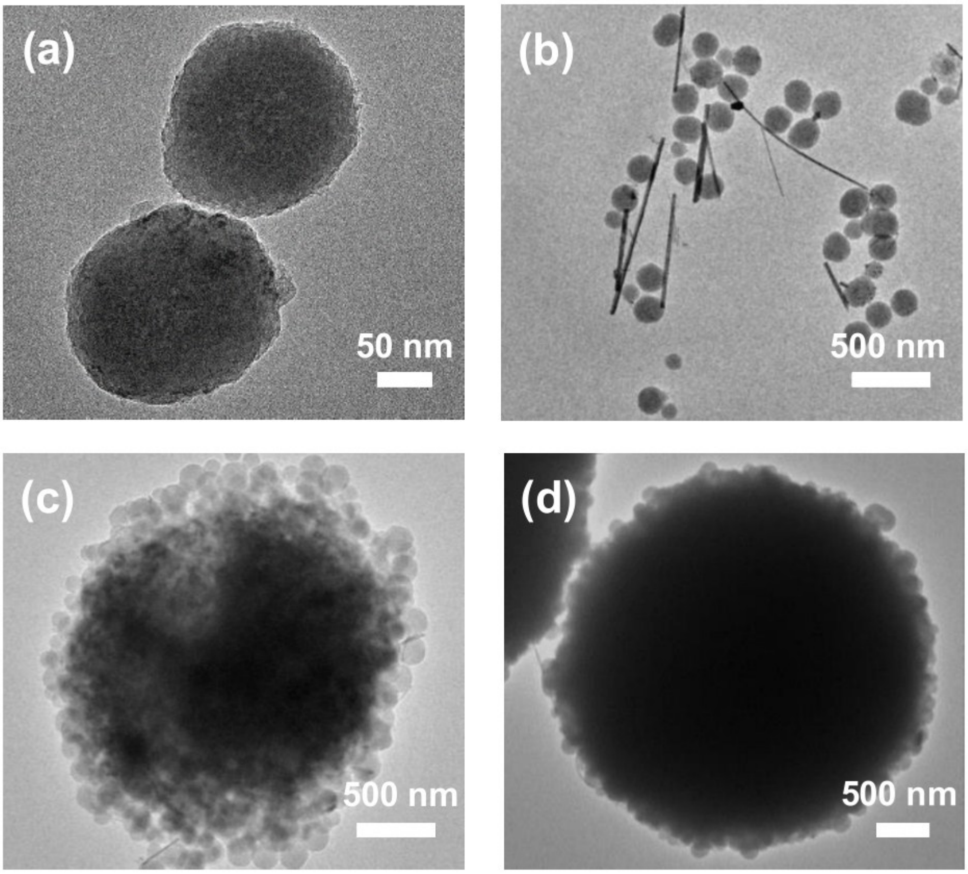

Figure S2 TEM images of the morphology changes of the W-PDA superstructure from SiO_2@C solid spheres during the whole assembly process.

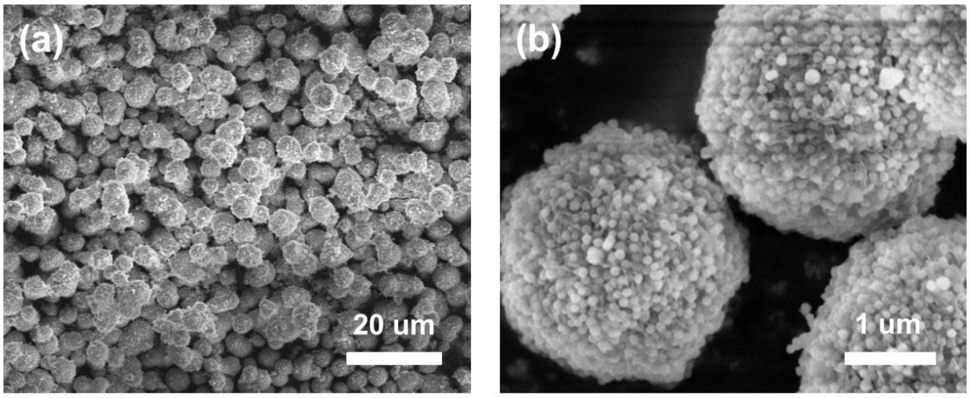

Figure S3 SEM images of the W-PDA superstructure using SiO_2@C solid spheres as the blocks.

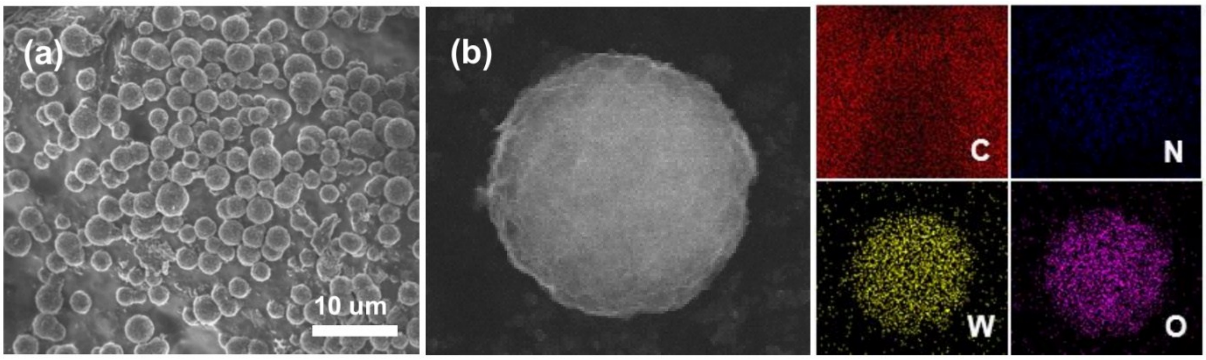

Figure S4 SEM and SEM-EDS element mapping images of the WO_2/N-PC superstructure.

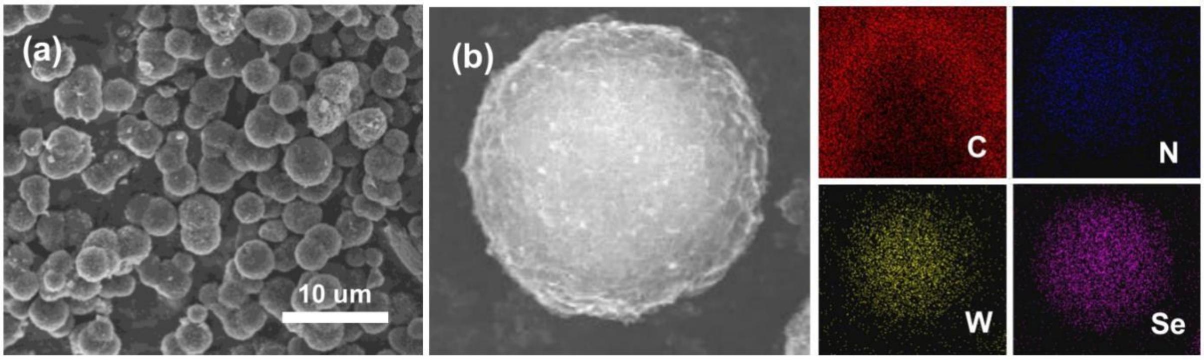

Figure S5 SEM and SEM-EDS element mapping images of the WSe_2/N-PC superstructure.

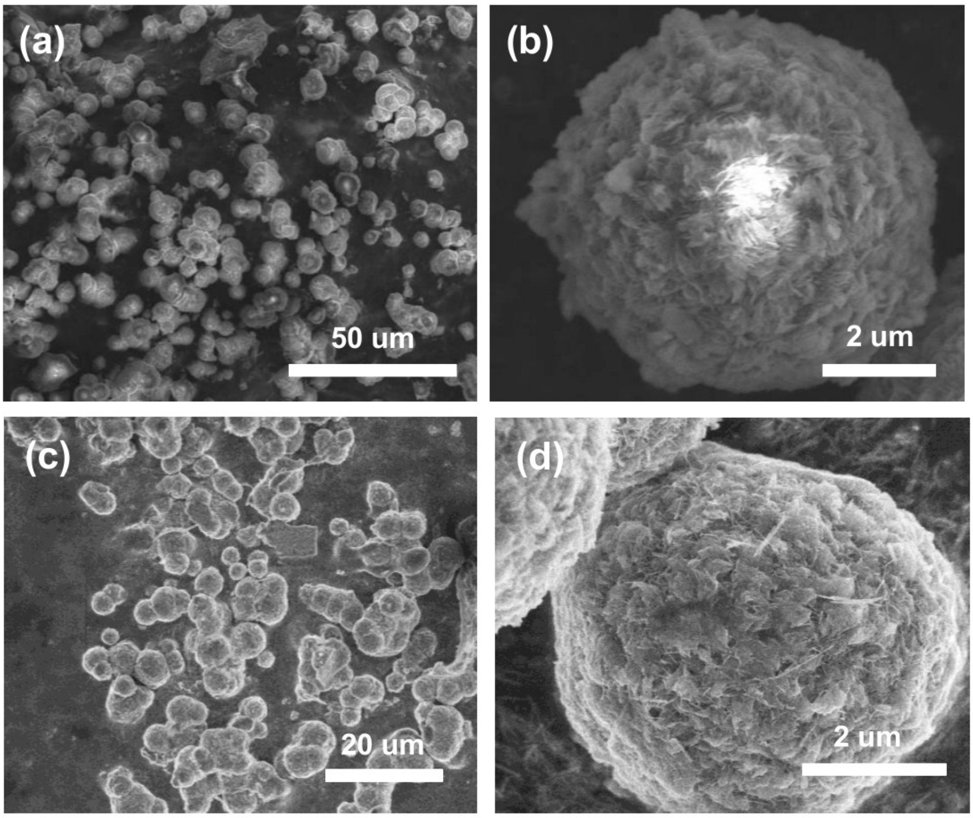

Figure S6 SEM images of (a and b) W-PDA precursor without adding SiO_2@C blocks, (c and d) WO_2/N-C microsphere.

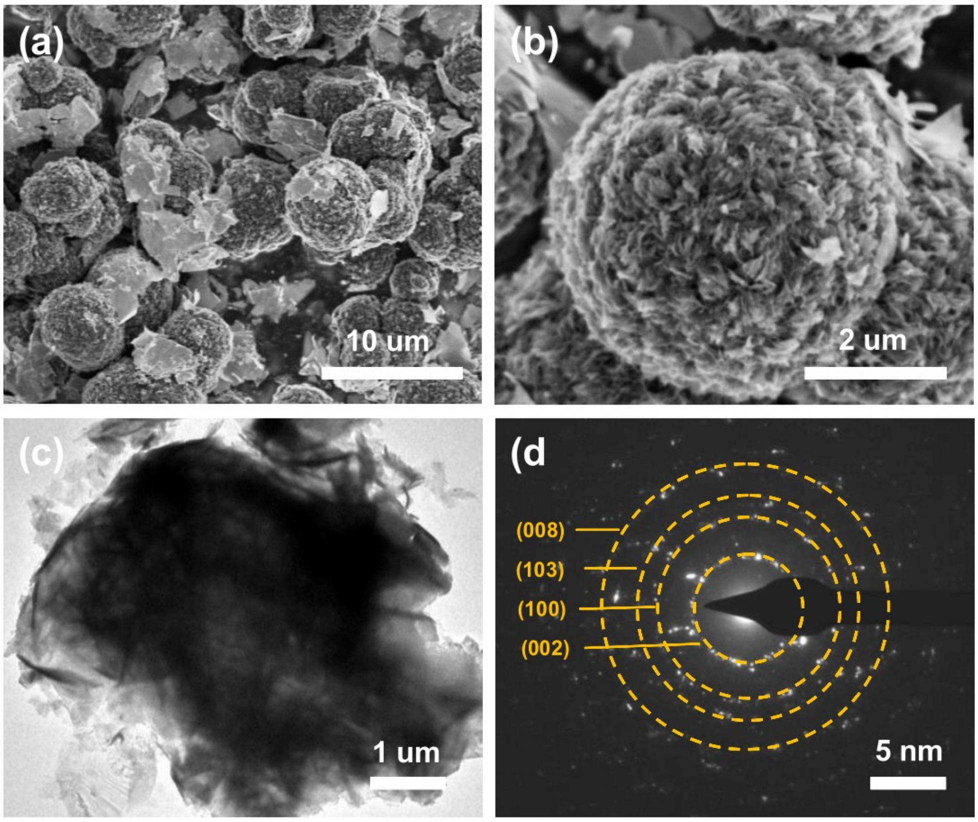

Figure S7 SEM, TEM, and SAED images of WSe_2/N-C microsphere.

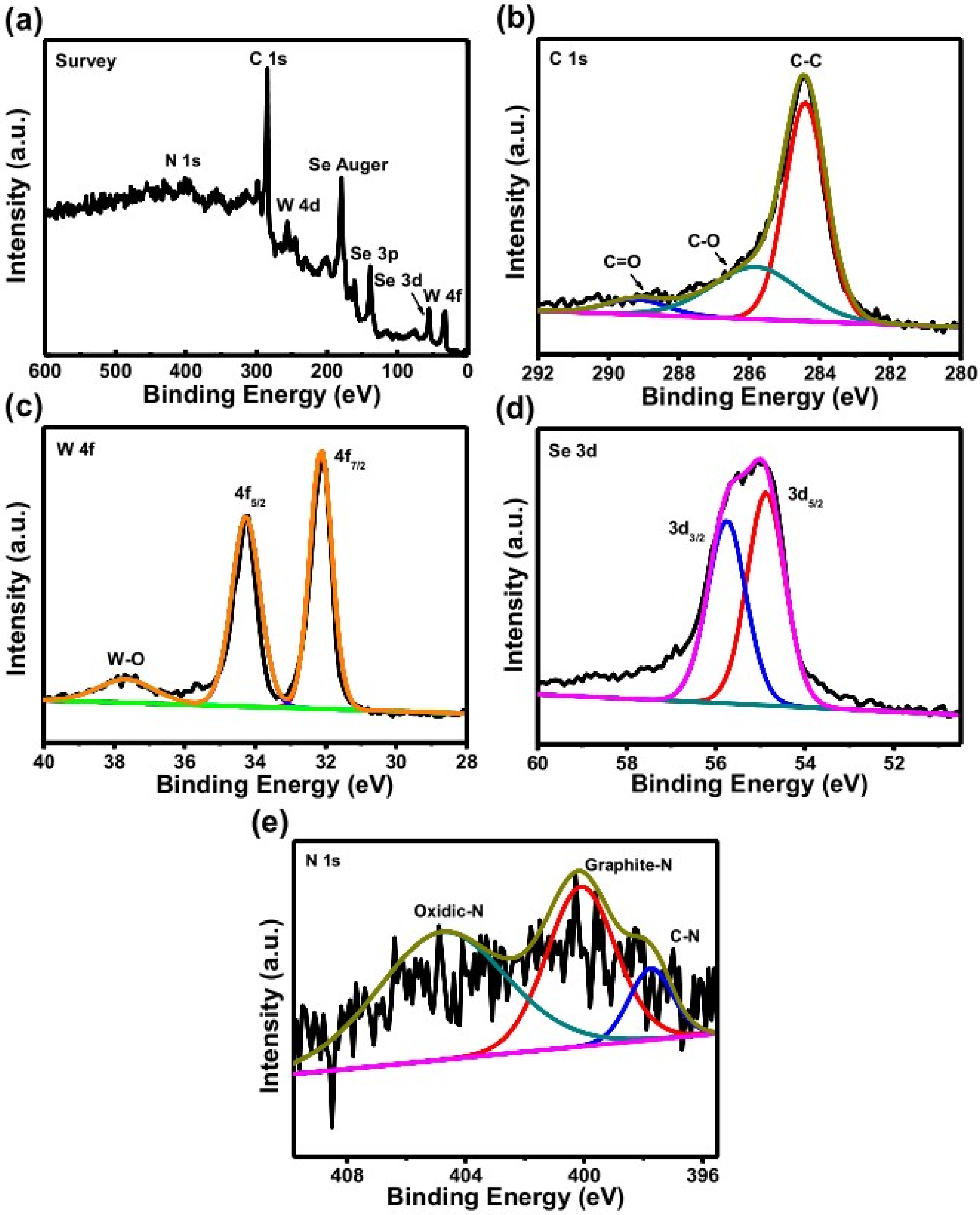

Figure S8 XPS spectra of WSe_2/N-PC: (a) survey spectrum, (b) C 1s spectrum, (c)W4f spectrum, (d) Se 3d spectrum, and (e) N 1s spectrum.

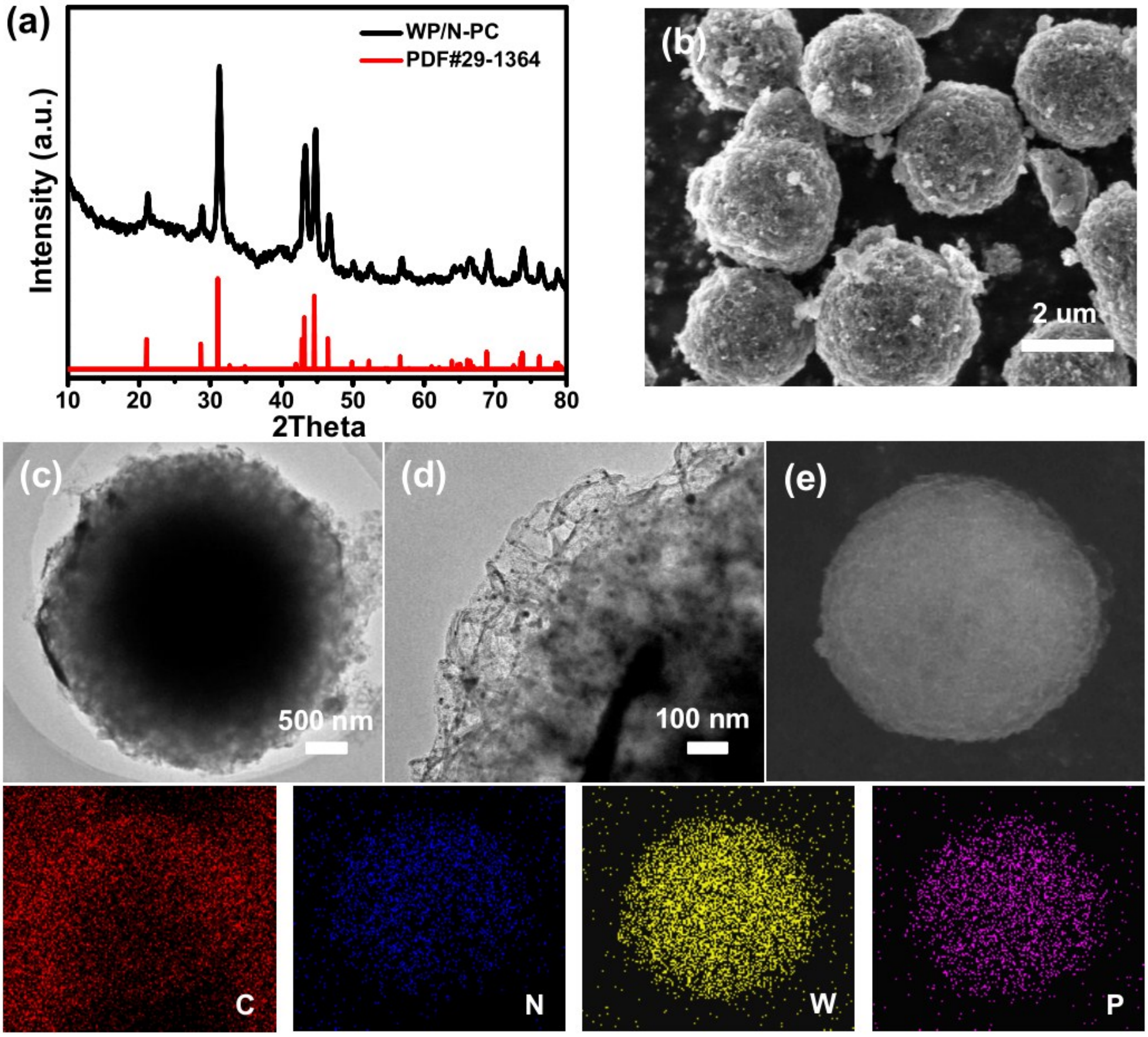

Figure S9 (a) XRD pattern; (b) SEM image; (c and d) TEM images and (e) EDS element mapping images of WP/N-PC superstructure.

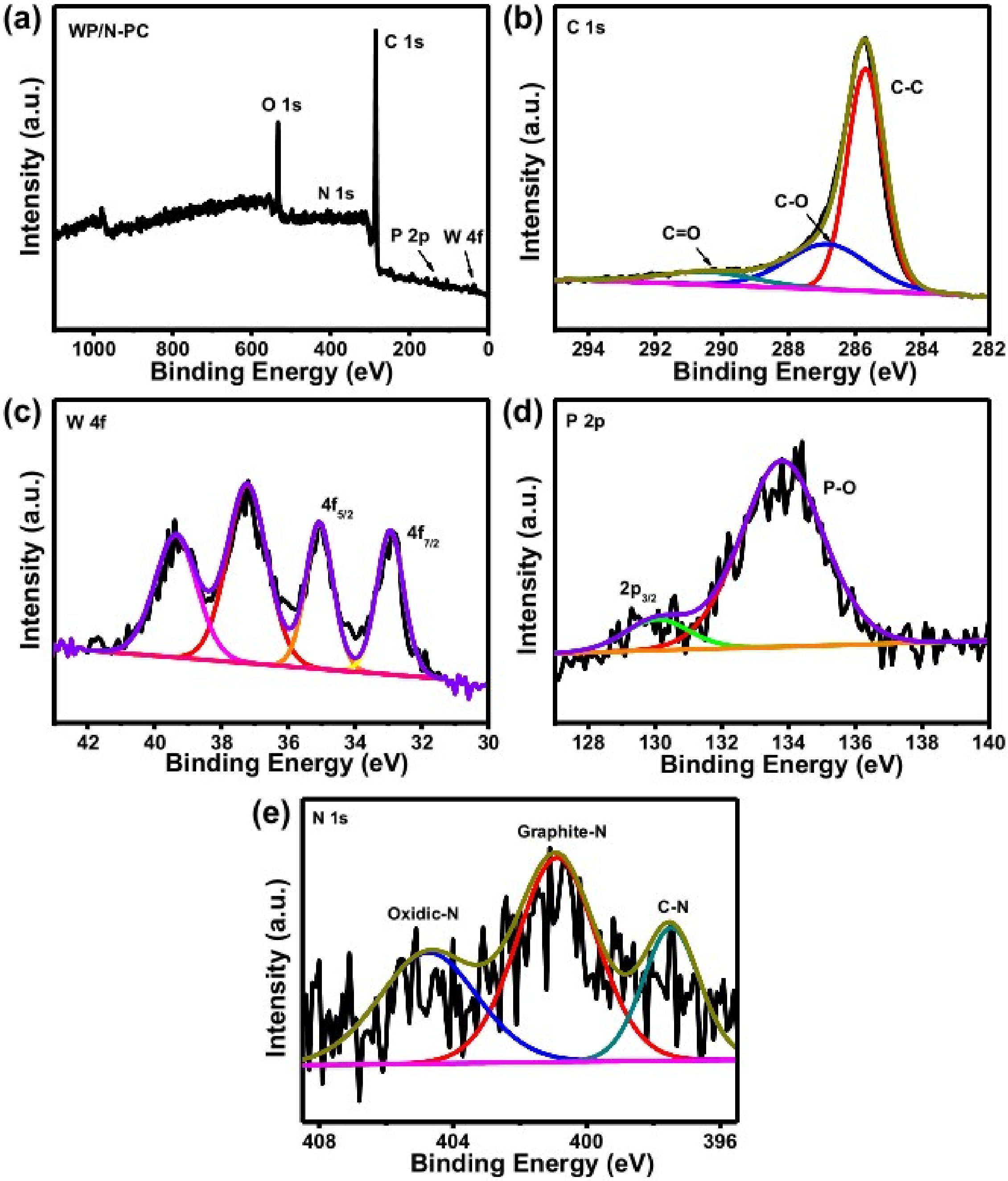

Figure S10 XPS spectra of WP/N-PC: (a) survey spectrum, (b) C 1s spectrum, (c) W4f spectrum, (d) P 2p spectrum, and (e) N 1s spectrum.

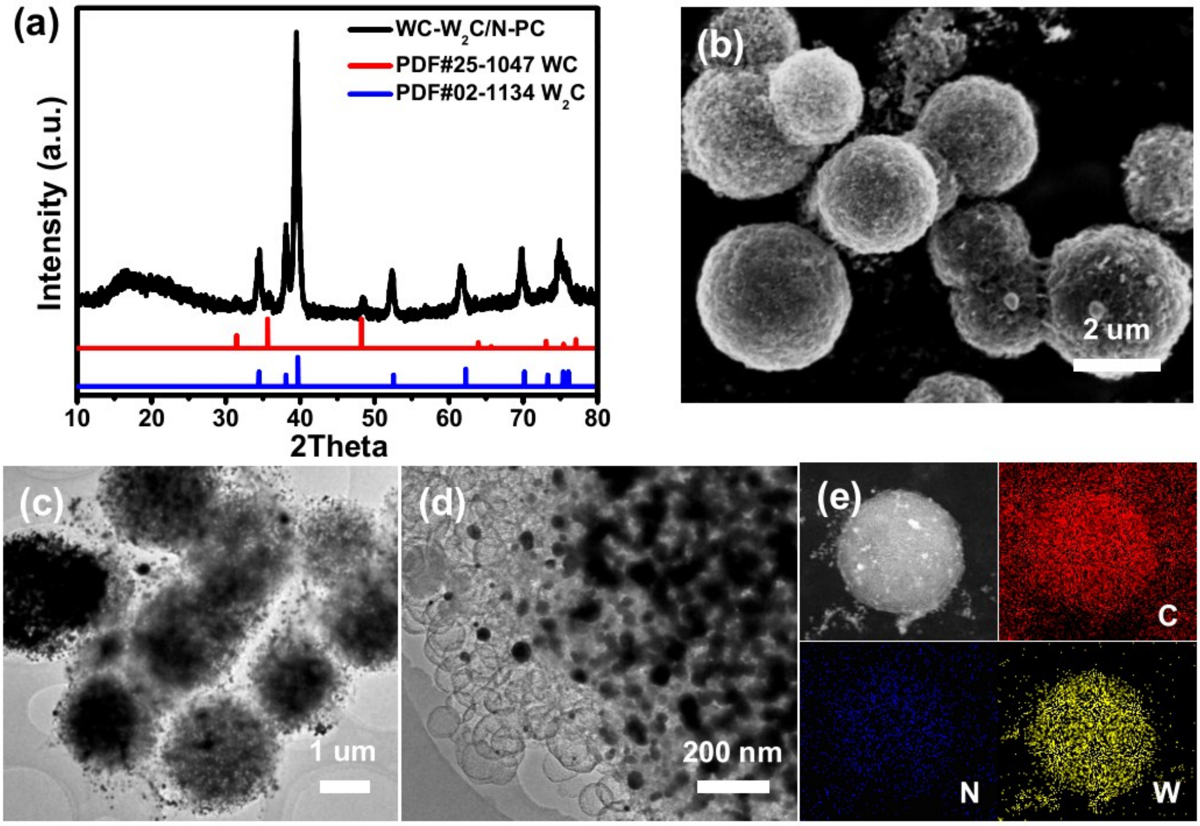

Figure S11 (a) XRD pattern; (b) SEM image; (c and d) TEM images and (e) EDS element mapping images of WC-W_2C/N-PC superstructure.

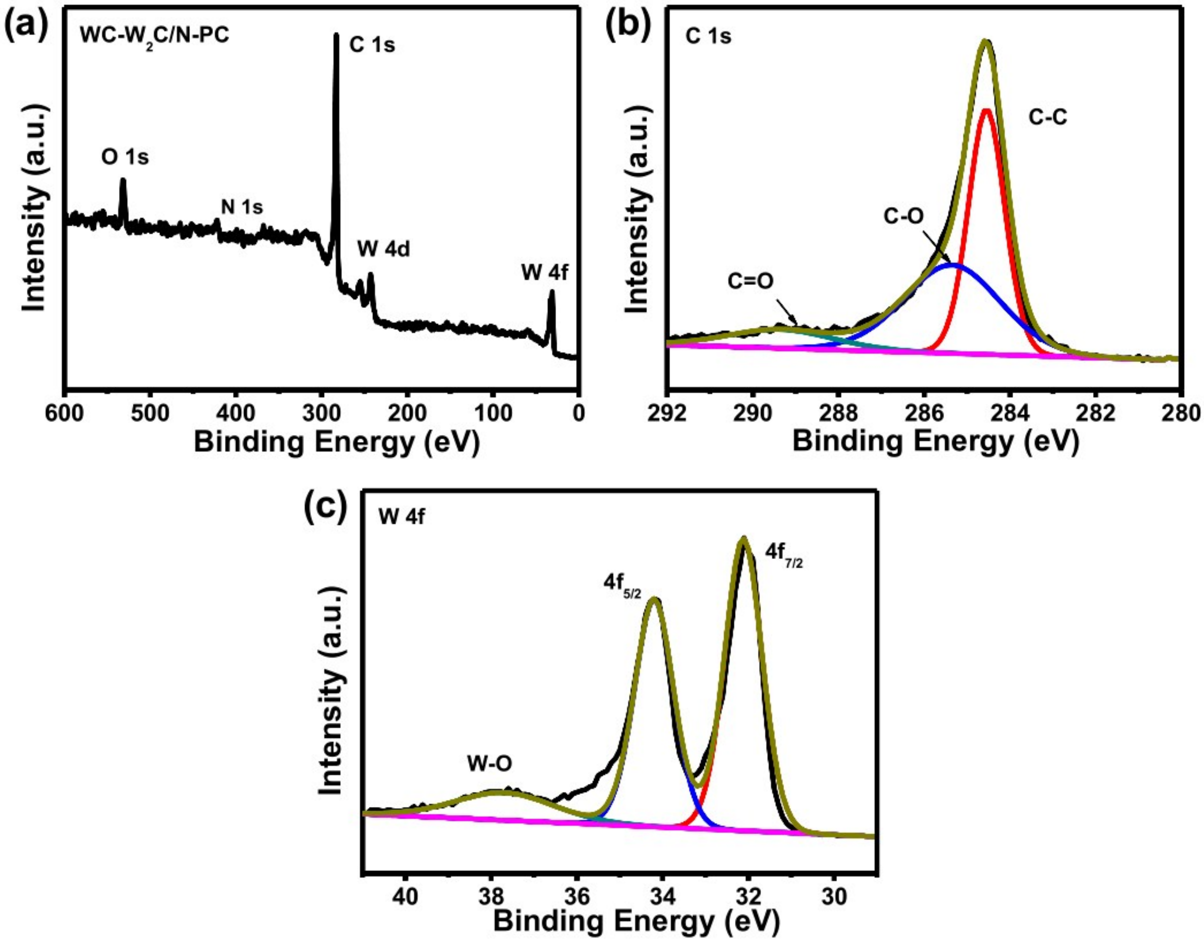

Figure S12 XPS spectra of WC-W_2C/N-PC: (a) survey spectrum, (b) C 1s spectrum, (c) W4f spectrum.

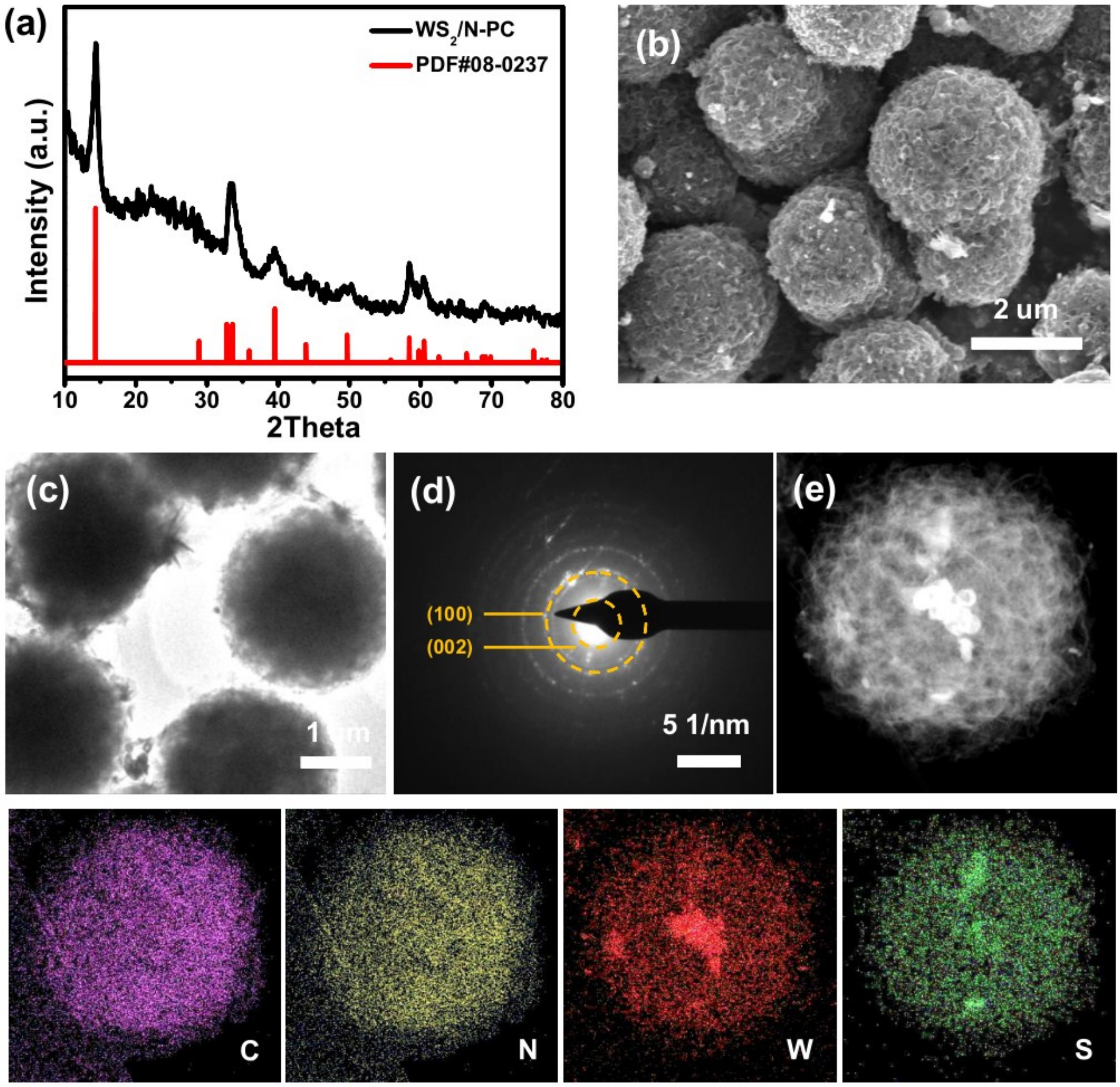

Figure S13 (a) XRD pattern; (b) SEM image; (c) TEM images; (d) SAED pattern and (e) TEM element mapping images of WS_2/N-PC superstructure.

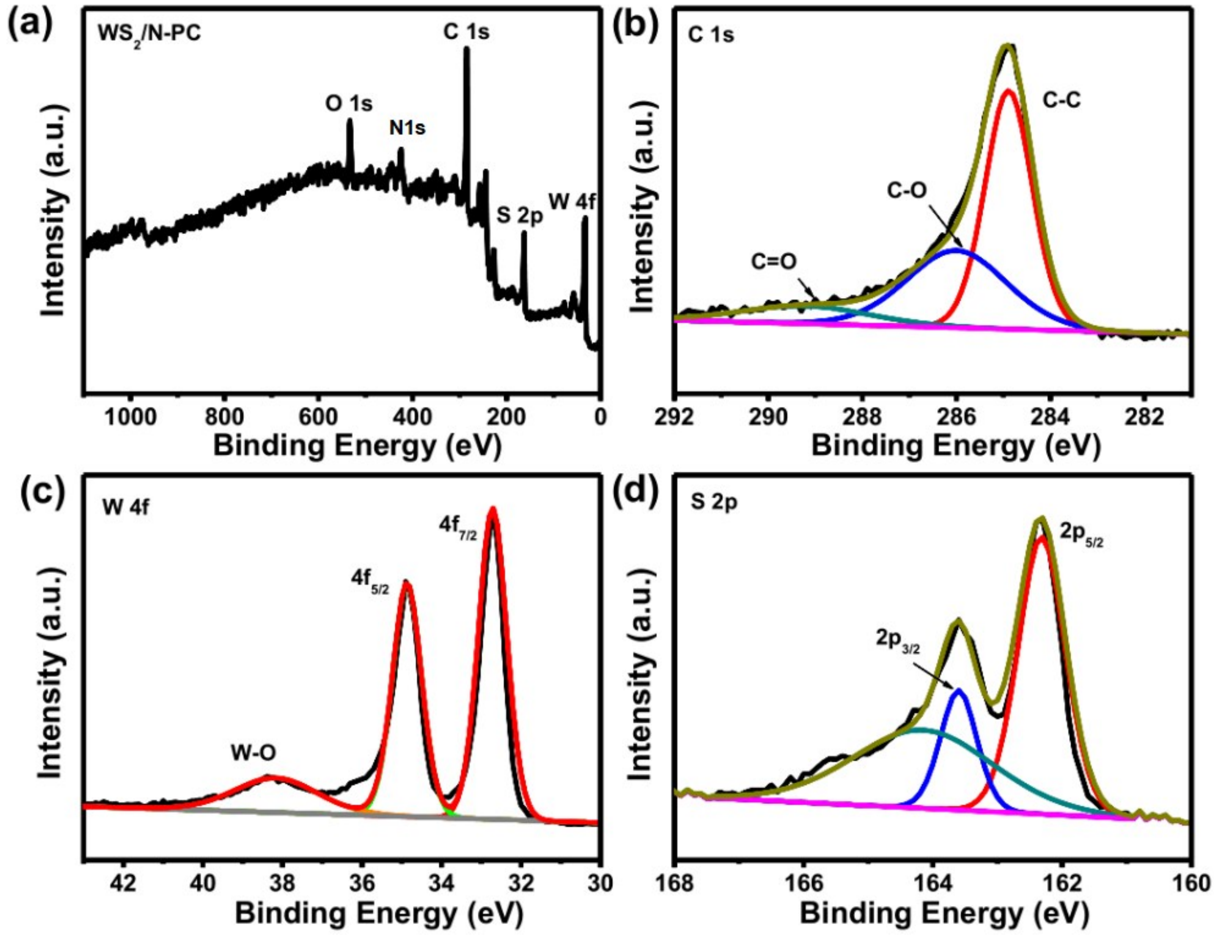

Figure S14 XPS spectra of WS_2/N-PC: (a) survey spectrum, (b) C 1s spectrum, (c) W4f spectrum, (d) S 2p spectrum.

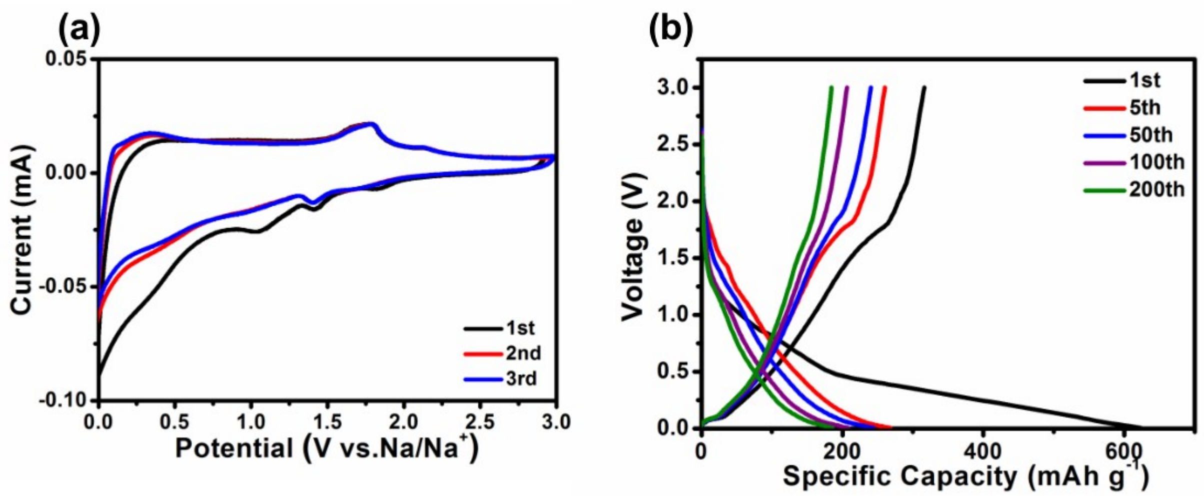

Figure S15 Electrochemical characterizations of SIBs: (a) CV profiles of WSe_2/N-C electrode at a scan rate of 0.2 mV s^{-1}; (b) Discharge and charge profiles of WSe_2/N-C electrode.

Table 1 Electrochemical performance comparision of this work versus WSe_2-based anode materials with different structures for SIBs.

Materials	Current density	Specific capacity, cycle number	Ref.
WSe_2-N/PC superstructure	0.1 A g^{-1} 0.2 A g^{-1} 0.8 A g^{-1}	390 mAh g^{-1}, 200 cycles 316 mAh g^{-1}, 400 cycles 184 mAh g^{-1}, 400 cycles	This work
WSe_2-15-PInanosheets	0.03 A g^{-1}	238 mAh g^{-1}, 100 cycles	14
Bulk WSe_2	0.1 A g^{-1}	190 mAh g^{-1}, 30 cycles	17
Nanostructured WSe_2/C	0.2 A g^{-1}	270 mAh g^{-1}, 50 cycles	29
WSe_2-G	0.1 A g^{-1}	303 mAh g^{-1}, 80 cycles	37
WSe_2 onions	0.1 A g^{-1}	383 mAh g^{-1}, 40 cycles	38

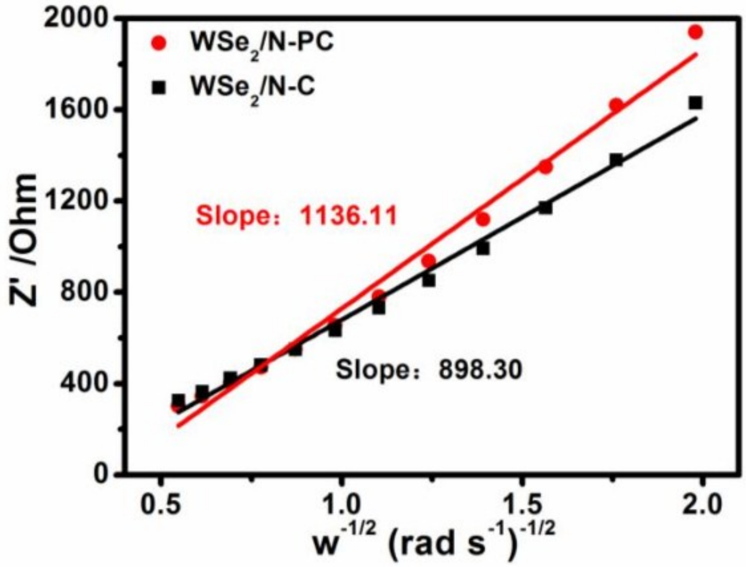

Figure S16 The relationship between Z′ and $\omega^{-1/2}$ in the low frequency region of WSe_2/N-PC and WSe_2/N-C electrodes after 3 cycles for SIBs.

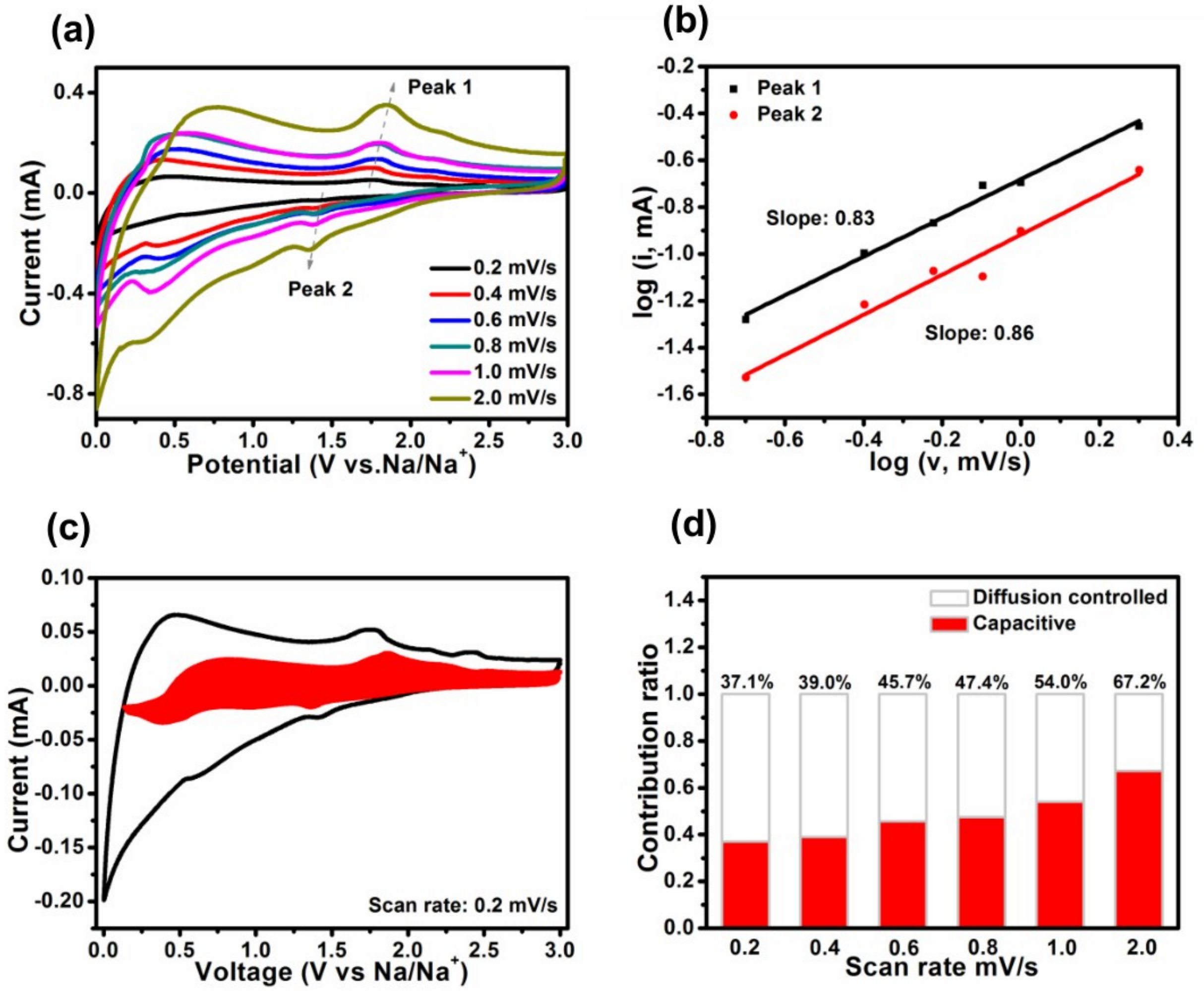

Figure S17 Sodium storage behaviors of WSe_2/N-C: (a) CV curves at different scan rates from 0.2 to 2.0 mV s^{-1}; (b) Log i vs. log v plots at oxidation and reduction state; (c) Capacitive- and diffusion-controlled contribution to charge storage at 0.2 mV s^{-1}; (d) Normalized contribution ratio of capacitive- and diffusion-controlled capacities at different scan rates.

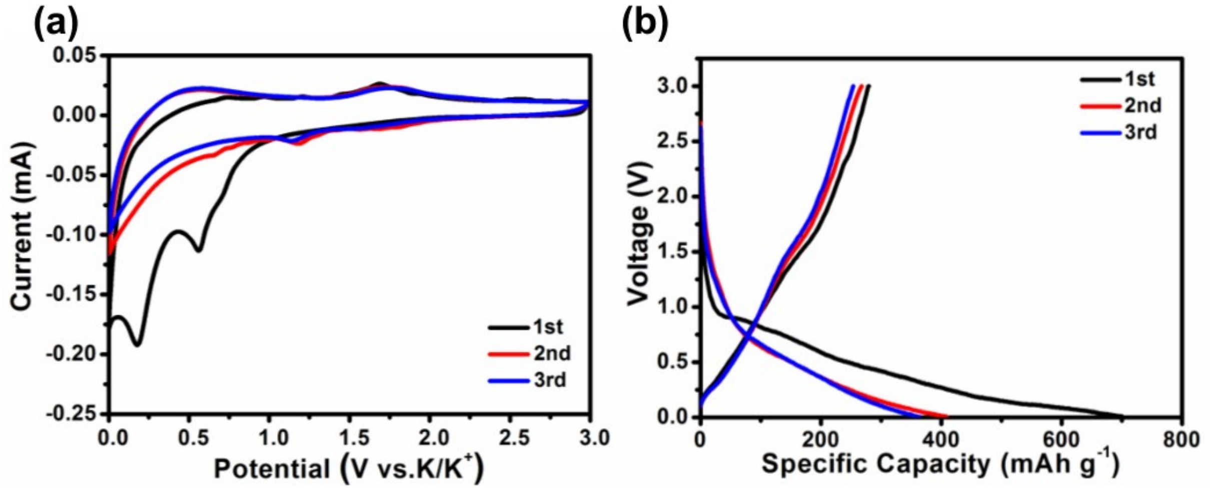

Figure S18 Electrochemical characterizations of PIBs: (a) CV profiles of WSe_2/N-C electrode at a scan rate of 0.2 mV s^{-1}; (b) Discharge and charge profiles of WSe_2/N-C electrode.

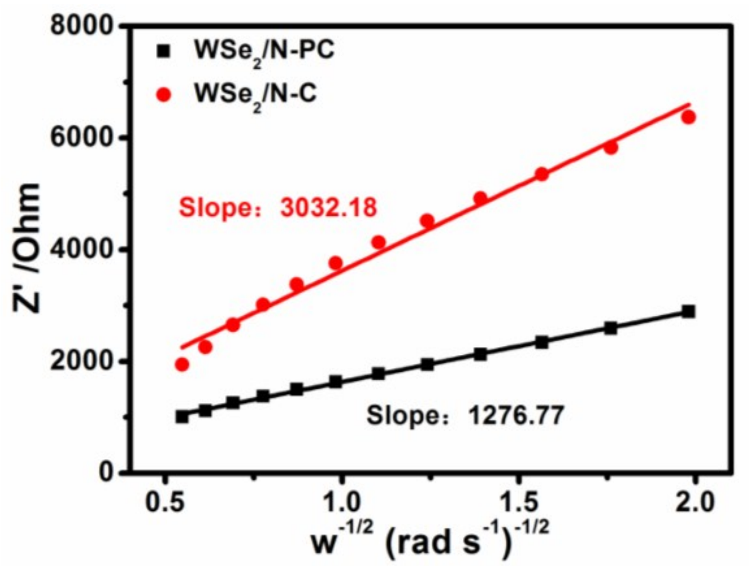

Figure S19 The relationship between Z′ and $\omega^{-1/2}$ in the low frequency region of WSe_2/N-PC and WSe_2/N-C electrodes after 3 cycles for PIBs.

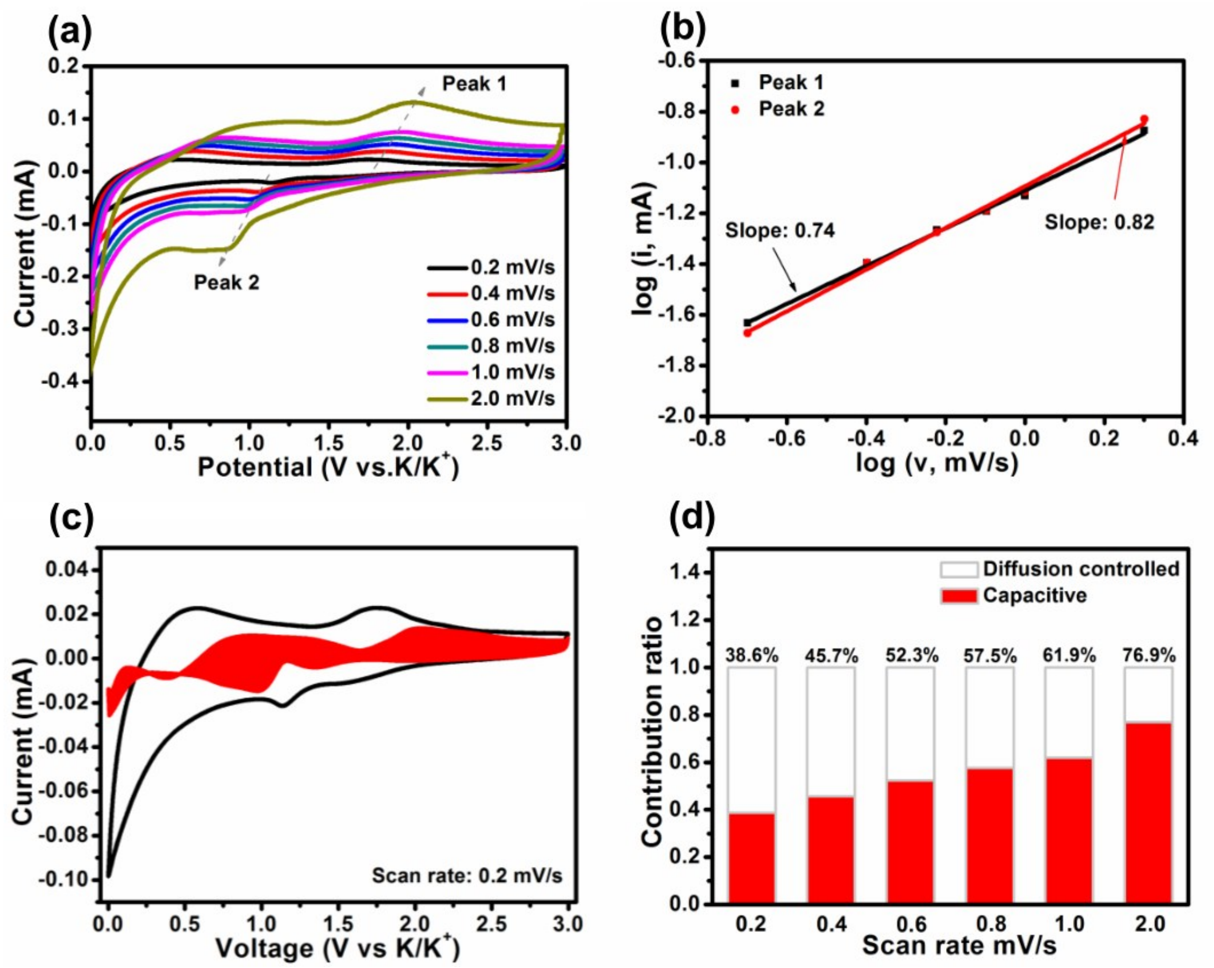

Figure S20 Potassium storage behaviors of WSe_2/N-C: (a) CV curves at different scan rates from 0.2 to 2.0 mV s^{-1}; (b) Log i vs. log v plots at oxidation and reduction state; (c) Capacitive- and diffusion-controlled contribution to charge storage at 0.2 mV s^{-1}; (d) Normalized contribution ratio of capacitive- and diffusion-controlled capacities at different scan rates.

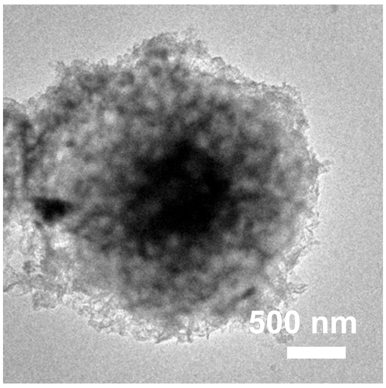

Figure S21 TEM image of WSe_2/N-PC electrode after rate performance for potassium storage.